THE JOURNAL OF BIOLOGICAL CHEMISTRY
Vol. 276, No. 48, Issue of November 30, pp. 45001–45008, 2001

Printed in U.S.A.

Structural Model of the Catalytic Core of Carnitine Palmitoyltransferase I and Carnitine Octanoyltransferase (COT)

MUTATION OF CPT I HISTIDINE 473 AND ALANINE 381 AND COT ALANINE 238 IMPAIRS THE CATALYTIC ACTIVITY*

Received for publication, July 23, 2001, and in revised form, September 6, 2001
Published, JBC Papers in Press, September 10, 2001, DOI 10.1074/jbc.M106920200

Montserrat Morillas‡, Paulino Gómez-Puertas§, Ramón Roca§, Dolors Serra, Guillermina Asins, Alfonso Valencia§, and Fausto G. Hegardt¶

From the Department of Biochemistry and Molecular Biology, School of Pharmacy, University of Barcelona, E-08028 Barcelona, Spain and §Protein Design Group, National Center for Biotechnology (Consejo Superior de Investigaciones Científicas), Cantoblanco, Madrid E-28049, Spain

Carnitine palmitoyltransferase I (CPT I) and carnitine octanoyltransferase (COT) catalyze the conversion of long- and medium-chain acyl-CoA to acylcarnitines in the presence of carnitine. We propose a common three-dimensional structural model for the catalytic domain of both, based on fold identification for 200 amino acids surrounding the active site through a threading approach. The model is based on the three-dimensional structure of the rat enoyl-CoA hydratase, established by x-ray diffraction analysis. The study shows that the structural model of 200 amino acids of the catalytic site is practically identical in CPT I and COT with identical distribution of 4 β-sheets and 6 α-helices. Functional analysis of the model was done by site-directed mutagenesis. When the critical histidine residue 473 in CPT I (327 in COT), localized in the acyl-CoA pocket in the model, was mutated to alanine, the catalytic activity was abolished. Mutation of the conserved alanine residue to aspartic acid, A381D (in CPT I) and A238D (in COT), which are 92/89 amino acids far from the catalytic histidine, respectively (but very close to the acyl-CoA pocket in the structural model), decreased the activity by 86 and 80%, respectively. The K_m for acyl-CoA increased 6–8-fold, whereas the K_m for carnitine hardly changed. The inhibition of the mutant CPT I by malonyl-CoA was not altered. The structural model explains the loss of activity reported for the CPT I mutations R451A, W452A, D454G, W391A, del R395, P479L, and L484P, all of which occur in or near the modeled catalytic domain.

Carnitine palmitoyltransferase I (CPT I[1]; EC 2.3.1.21) and carnitine octanoyltransferase (COT; EC 2.3.1.137) facilitate the transport of long and medium chain acyl-CoA in mitochondria and peroxisomes, respectively. Both carnitine acyltransferases facilitate the generation of energy by β-oxidation of fatty acids in the organella in which they are present. Mammalian tissues express two different isoforms of CPT I, a liver isoform (L-CPT I) (1, 2) and a heart/skeletal muscle isoform (M-CPT I) (3, 4). As an enzyme that catalyzes the first rate-limiting step in β-oxidation, CPT I is tightly regulated by its physiological inhibitor malonyl-CoA. In regulating CPT I, malonyl-CoA confers the ability to signal to the cell the availability of lipid and carbohydrate fuels (5). CPT I has a critical metabolic role in general metabolism in heart, liver, and β-cells of the pancreas and is a potential target for the treatment of metabolic disorders involving diabetes and coronary heart disease. Peroxisomal COT is also inhibited in physiological conditions by malonyl-CoA (6) but to a lesser extent than CPT I. Other enzymes of the family, which are not regulated by malonyl-CoA, are CPT II, which catalyzes long-chain acyl-CoA in the mitochondria, and carnitine acetyltransferase, which has acetyl-CoA as substrate.

These enzymes have recently generated much interest, especially the spatial organization of CPT I in the mitochondrial outer membrane. CPT I is an integral membrane protein, and both the N and C termini project to the cytosol, since it has two trans-membrane segments within the first 130 N-terminal residues of its primary sequence (7). Interaction between amino acids from the N and C termini may determine the kinetic characteristics of the enzyme, not only in the inhibitory effect of malonyl-CoA but also in the catalytic activity (8). COT appears not to be an integral protein of peroxisomes. Sequence alignment between CPT I and COT shows that COT lacks the first 152 amino acid residues, which indicates that it has no transmembrane regions. However, the two show high sequence identity, which suggests a common genetic origin (9).

Although several attempts have been made to identify the malonyl-CoA site, few data are available on the structure of the catalytic site of carnitine acyltransferases. It has been proposed that a histidine residue is critical in catalysis (10). Site-directed mutagenesis experiments have demonstrated an essential catalytic role for histidine 372 in CPT II (11) and the homologous histidine 327 in COT (12). However the role of a histidine in catalysis has been questioned for both CPT I and COT (13, 14). Dai *et al.* observed that overexpressed CPT I in yeast treated with diethylpyrocarbonate did not decrease the enzyme activity at variance with wild type rat mitochondria, although differences in the folding of CPT I in yeast and in rat liver could lead to an alternative interpretation.

Other amino acids residues have been also implicated in

* This study was supported by Dirección General de Investigación Científica y Técnica, Spain, Grant PB95-0012; by Ajuts de Suport als Grups de Recerca de Catalunya Grants 1999SGR-0075 and 2001SGR00129 (to F. G. H.); and by a grant of the Marató de TV3. The costs of publication of this article were defrayed in part by the payment of page charges. This article must therefore be hereby marked "*advertisement*" in accordance with 18 U.S.C. Section 1734 solely to indicate this fact.

‡ Recipient of a fellowship from the Ministerio de Educación y Cultura, Dirección General de Enseñanza Superior, Spain.

¶ To whom correspondence should be addressed: Dept. of Biochemistry, School of Pharmacy, Avda. Diagonal 643, E-08028 Barcelona, Spain. Tel.: 34 93 402 4523; Fax: 34 93 402 4520; E-mail: hegardt@farmacia.far.ub.es.

[1] The abbreviations used are: CPT, carnitine palmitoyltransferase; COT, carnitine octanoyltransferase; PCR, polymerase chain reaction.

catalysis. Mutation of several conserved arginines (Arg^{388}, Arg^{451}) and tryptophans (Trp^{391}, Trp^{452}) comprised between amino acids 381 and 481 of CPT I decreased enzyme activity (13). These authors suggested that this segment could be the putative palmitoyl-CoA binding site of CPT I. In this fragment, mutants D376A and D464A in rat CPT II were completely inactive (11). As to the carnitine binding site, arginine 505 in beef COT, which lies outside the proposed palmitoyl-CoA binding site, has been implicated (15).

In this study, we propose three-dimensional models of the catalytic site comprising amino acids 368–568 in CPT I and 226–417 in COT. These models were made using an integrative approach of several threading procedures taking into account different parameters such as solvatation potentials, contacts, environment-specific substitution tables, and structure-dependent gap penalties. The fold recognition analysis using these procedures showed a common template for the catalytic site of the carnitine/choline acyltransferase family of proteins, corresponding to the structure of the enoyl-CoA hydratase enzyme (Protein Data Bank entry 2dub; Ref. 16); this motif was also found in CPT I and COT. The three-dimensional models for CPT I and COT are practically identical and show a common architecture for the catalytic site. Site-directed mutagenesis indicated that CPT I His^{473} and COT His^{327} are the catalytic residues. These histidines are located near the thioester bond in the acyl-CoA, which is broken in catalysis. Mutation of CPT I A381 and COT A238, located close to the catalytic histidine decreased the enzyme activity by 80–86% without modifying the sensitivity to malonyl-CoA.

EXPERIMENTAL PROCEDURES

Fold Recognition and Model Building—Sequences homologous to rat CPT I and COT were obtained using BLAST (17). The sequences were aligned using ClustalW (18). Secondary structure analysis of the sequences was performed using the public servers PHD (19), Jpred (20), and Psi-Pred (21).

Protein structure predictions were performed using the threading programs: Threader2 and FUGUE. Threader2 (22) is based on solvatation potentials and contacts (pair potentials) and can detect the correct fold in the absence of homology. FUGUE (23) uses environment-specific substitution tables and a structure-dependent gap penalty to detect remote structural homologues. The models predicted by the two procedures were compared and evaluated using information from the publicly available structural classification data bases CATH (24), FSSP (25), and SCOP (26).

When the template structure had been chosen, the three-dimensional models of rat CPT I and COT were obtained using the program Swiss-Pdb Viewer and the SWISS-MODEL server facilities (27–30). The atomic coordinates of the monomeric structure of the rat enoyl-CoA hydratase used as template were obtained from the Protein Data Bank (entry 2dub, chain E).

The models of the active site-surrounding regions of CPT I and COT were validated using the programs ProsaII (31), WHAT-CHECK (32), from WHAT-IF (33), and PROCHECK (34). Data from the analysis procedures as well as the template structure and the multiple alignment of the carnitine-choline acyltransferase family of proteins are available as supplementary information on the World Wide Web (www.cnb.uam.es/~pagomez/CPTI_COT).

Calculations and representation of electrostatics potentials were performed using GRASP (35). Ribbon plots were drawn with RASMOL (36).

Subfamily Conserved Residue Analysis (Tree Determinants)—Conserved differences between short-chain acyltransferases (choline or carnitine acetyltransferases) and long- and medium-chain acyltransferases (carnitine octanoyltransferase or palmitoyltransferases) were analyzed with the SequenceSpace algorithm (37, 38), using the multiple alignment of the carnitine-choline acyltransferase family of proteins as input.

Construction of Plasmids for Expression in Saccharomyces cerevisiae—For expression experiments, the fragment that encompassed nucleotides 103–2701, including the coding region of CPT I, was subcloned into the *S. cerevisiae* expression plasmid pYES2 (Invitrogen). A *Hin*dIII site (underlined) was introduced by PCR immediately 5′ of the ATG start codon of CPT I to enable cloning into the unique *Hin*dIII site of plasmid pYES2. A consensus sequence (in boldface type), optimized for efficient translation in yeast, was also introduced in the same PCR, using the forward primer CPTI*Hin*dIII.for (5′-TCG AT**A AGC TTA AA**AT GGC AGA GGC TCA CCA AGC TG-3′) and the reverse primer CPTI911.rev (5′-GCT GCC TGG ATA TGG GTT GG-3′). PCR products were digested with *Hin*dIII and *Kpn*I and ligated to the pYES2 plasmid. The plasmid was digested with *Kpn*I and *Eco*RI and ligated with the CPT I fragment *Kpn*I-*Eco*RI (nucleotides 660–2701), producing pYESCPTIwt.

Plasmids pYESCOTwt and $pYESCOT^{H327A}$ were obtained as previously described (12).

Construction of Site-directed Mutants—Plasmid pYESCPTIwt was used for site-directed mutagenesis of histidine 473 to alanine by the asymmetric PCR method (39). The mutated megaprimer fragment was obtained using the forward primer CPT1182.for (5′-GCA GCA GAT GCA GCA GAT CC-3′) and the reverse primer H473A.rev (5′-CCC AGG AGG CCT CTG CAT TTA TGC C-3′ (the mutated nucleotides are underlined). This megaprimer fragment was used together with the reverse primer CPT1878.rev (5′ GGC CTC ATA TGT GAG GC 3′) to obtain a PCR-amplified fragment which, after digestion with *Pst*I, was subcloned to obtain the plasmid $pYESCPTI^{H473A}$.

Mutants A381D of CPT I and A238D of COT were constructed using the QuickChange PCR-based mutagenesis procedure (Stratagene) with the pYESCPTIwt and pYESCOTwt plasmid as template. Primer 5′-GAG GCC AAG CTG GAC GCC CTC ACT GCT GC-3′ was used to construct $pYESCPTI^{A381D}$, and primer 5′-GTT GGG CCC AGT ATA GAC GCA TTA ACC AGT GAG GAG C-3′ was used to construct $pYESCOT^{A238D}$. The appropriate substitutions and the absence of unwanted mutations were confirmed by sequencing the inserts in both directions with an Applied Biosystems 373 automated DNA sequencer.

Expression of CPT I and COT in S. cerevisiae—For expression in yeast cells, the wild-type YPH499 (*MAT a ura3–52 leu2-Δ1 ade2–101 lys2–801 his3- Δ200 trp1- Δ63*) was transformed with different constructs (see above) using a modification of previously described methods (40). Positive colonies were selected and grown in complete minimal medium lacking uracil, CM(−ura), with 2% glucose as a carbon source (41).

For COT expression, extracts were obtained as described in Ref. 12. For CPT I expression, appropriate amounts (~15 ml) of the glucose cultures were inoculated in 400 ml of CM(−ura) plus 2% lactate and grown to an A_{660} of 1. 2% of galactose was added and growth was continued for 20 h at 30 °C to induce expression. Cells were recovered by centrifugation at 2000 × *g* for 5 min at 4 °C, washed twice in distilled water, resuspended in a small amount of water, transferred to a smaller tube, centrifuged at 800 × *g* for 5 min at 4 °C, and resuspended in buffer with 10 mM Hepes, pH 7.4, 1 mM EDTA, and 10% glycerol supplemented with 1 mM phenylmethylsulfonyl fluoride, 2 μg/ml leupeptin, 1 μg/ml pepstatin, and 0.5 μM benzamidine. The same volume of cold, acid-washed glass beads (Sigma; catalog no. G-9268) was added to each sample, and cells were disrupted by vigorous vortexing (five pulses of 1 min; samples were kept on ice for 1 min after each pulse). Homogenates were then centrifuged at 800 × *g* for 5 min at 4 °C to remove glass beads and cell debris. This crude extract was further centrifuged at 15,000 × *g* for 45 min at 4 °C to obtain a mitochondrial extract, which was immediately frozen and stored at −70 °C.

Determination of Carnitine Acyltransferase Activity—Carnitine acyltransferase activity was determined by the radiometric method as previously described (12). The substrates were palmitoyl-CoA (for CPT I) or decanoyl-CoA (for COT) and L-[*methyl*-^{3}H]carnitine. The protein sample was ~10 μg for CPT I and ~2 μg for COT.

The K_m of CPT I for carnitine was measured at a fixed 135 μM palmitoyl-CoA concentration. The K_m of CPT I for palmitoyl-CoA, was measured at a fixed carnitine concentration of 400 μM. The K_m of COT for carnitine was measured at a fixed decanoyl-CoA concentration of 50 μM. The K_m of COT for decanoyl-CoA was measured at a fixed carnitine concentration of 400 μM. Malonyl-CoA inhibition was assayed at increasing concentrations comprised between 1 and 200 μM.

Values reported are the means and S.D. of 3–5 determinations. All protein concentrations were determined using the Bio-Rad protein assay with bovine albumin as standard.

Immunological Techniques—An antibody against residues 428–441 of rat liver CPT I (which recognizes the C terminus of the enzyme), was kindly given by Dr. V. A. Zammit. *S. cerevisiae* protein extracts (100 μg for CPT I and 10 μg for COT) were subjected to SDS-polyacrylamide gel electrophoresis (SDS-PAGE). Electroblotting to nitrocellulose sheets was carried out for 2 h at 120 mA. Immunodetection of CPT I was performed using antiserum anti-L-CPTI (1:80 dilution), and the blots were developed with the ECL Western blotting system from Amersham

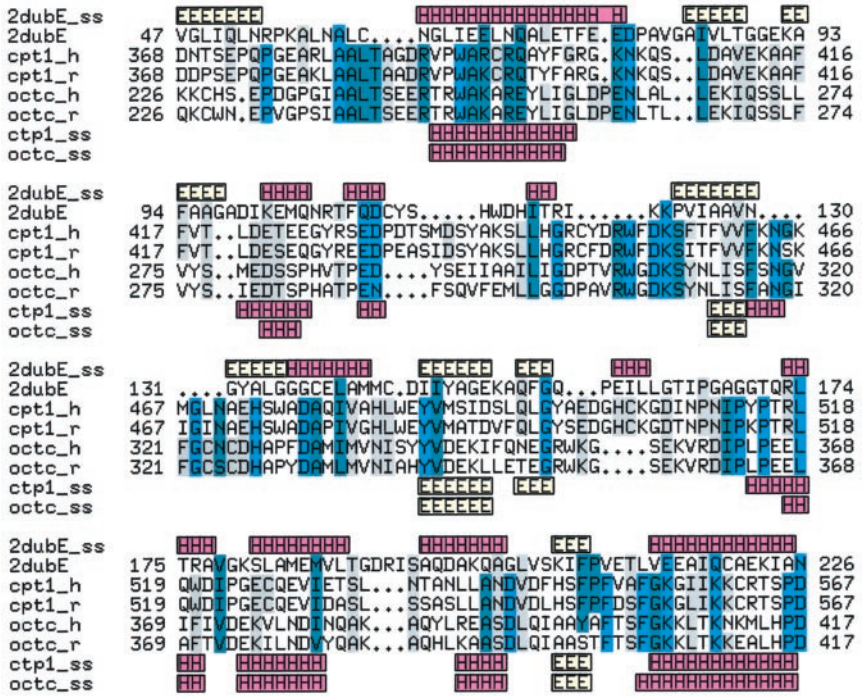

FIG. 1. **Structural alignment between the template enoyl-CoA hydratase sequence (2dubE) and carnitine palmitoyltransferases from human (cpt1_h) and rat (cpt1_r) and carnitine octanoyltransferases from rat (octc_r) and human (octc_h).** Secondary structure elements of 2dubE are represented (2dubE_ss) according to HSSP (47). *H*, α-helix; *E*, β-sheet. The secondary structure elements of the proposed models for rat CPT I and COT, derived from the PROMOD modeling algorithm results (43), are also represented. Residues are *colored* by conservation the Belvu version 2.8 program (by Erik Sonnhammer; available on the World Wide Web at www.sanger.ac.uk/~esr/Belvu.html).

Pharmacia Biotech. Inmunodetection of COT was performed as described previously (12).

RESULTS

Structural Model of CPT I and COT—We found 38 sequences including L and M isoforms of CPT I, CPT II, COT, CAT, and choline acetyltransferases from several organisms, that showed between 26 and 98% pairwise identity with rat CPT I and a conserved core surrounding the position corresponding to the conserved potential catalytic residue His^{473} (rat L-CPT I sequence numbering). This characteristic, in addition to the sequence identity values among all of the members of this family, suggests a common catalytic mechanism related to the acyl-CoA substrate, despite the different length of the acyl chain.

To obtain a structural model able to address some important questions related to the activity of these proteins, we have employed intensive threading approaches using two different programs, THREADER2 and FUGUE (see "Experimental Procedures") to find appropriate structural templates for CPT I (from liver and muscle), CPT II, COT, CAT, and choline acetyltransferase, all of them from humans and rodents. Due to the nature of the threading approaches and the average amino acidic length of the putative crystallized proteins used as templates, we decided to try to obtain a model, not of the whole proteins amino acid sequence, but only the central core surrounding the active site defined by the equivalent residues to the rat CPT I His^{473}. To this end, the ~200 amino acids surrounding His^{473} in rat and human CPT I (amino acids 368–567) and the equivalent positions of human and rodent members of the other subfamilies (*i.e.* human and rat COT amino acids 226–417, to a total of 12 protein sequences) were used to perform an extensive fold search.

A clear candidate emerged as fold template. The first six high scoring predictions for all of the sequences submitted to FUGUE included the enoyl-CoA hydratase fold (FUGUE code ech; Protein Data Bank code 2dub, chain E). Moreover, this fold occupies the first position in 8 of the 12 sequence results. THREADER2 gave a similar result, with the 2dubE fold, or equivalent, present in the first 10 positions of all of the predicted cases.

The structural pair alignments proposed by the threading algorithms between the template and the query sequences were analyzed, taking account of several characteristics, such as minimization of gaps, conservation of key positions, similarity of the hydrophobicity profile, and correspondence of the secondary structure. The best fit between all of these characteristics and the amino acid sequence implicit in the three-dimensional model of both the 2dubE template (amino acid residues 47–226) and the queries is shown in Fig. 1. The figure reports the final alignment used to perform the model building for the CPT I and COT proteins from humans and rats.

On the basis of this alignment, three-dimensional models of both CPT I and COT based on the 2dubE structure were built. Standard evaluation checks of both structures were performed using the WhatCheck (32), ProCheck (34), and ProsaII (31) procedures. In brief, the mathematical evaluation of the structures showed values included into the expected range for homology-based models, without relevant abnormalities. The amino acid backbone trace of the template structure and the two models are shown in Fig. 2 for comparison. The two models and the template have similar three-dimensional structure.

The position of the octanoyl-CoA molecule in the template structure can be used to approximately locate the corresponding substrates of CPT I and COT at their appropriate binding sites (Fig. 3). The obtained models for both proteins show a high structural similarity. The position of the catalytic residue (His^{473} in CPT I, His^{327} in COT) indicates that this amino acid is spatially located very close to the sulfur atom of the acyl-CoA substrate in both protein models. This result strongly supports the models since it offers a structural explanation of the catalytic activity in which this histidine position has been implicated (11, 12).

The inspection of the residues near the catalytic site spatially related to the catalytic histidine or proximal to the sulfur atom of the acyl-CoA molecule showed the presence of other amino acids in the vicinity. One of these positions corresponds to Ala^{381} in CPT I or Ala^{238} in COT (Fig. 3). The analysis of conserved differences between short-chain acyltransferases (choline or carnitine acetyltransferases) and long and medium length acyltransferases (CPT and COT) indicates that the

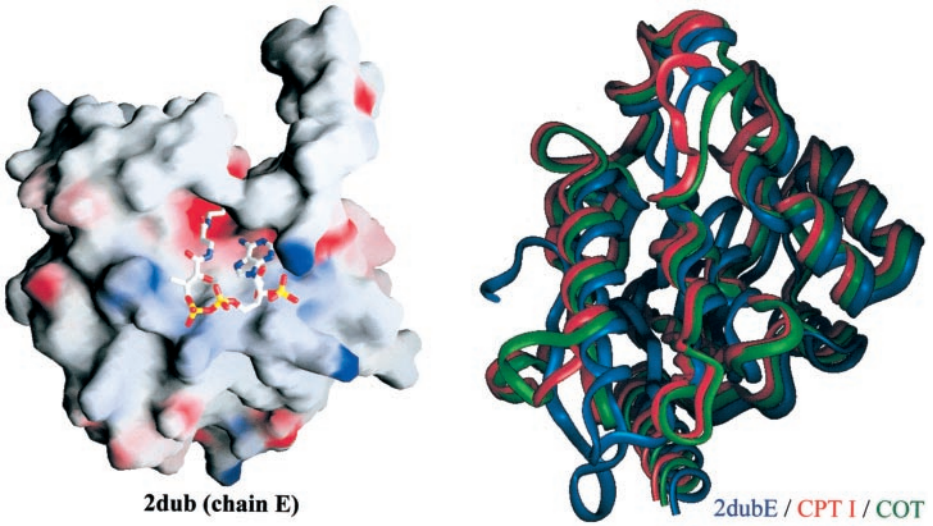

FIG. 2. **Structural template model alignment.** *Left*, solvent-accessible surface representation of the crystal structure of enoyl-CoA hydratase (2dub, chain E). The surface is *colored* according to the calculated electrostatic potential (negative (*red*) to positive (*blue*)). A molecule of octanoyl-CoA, co-crystallized with the protein, is also represented as "sticks." *Right*, superposition of the protein backbones of the 2dubE template (*blue*) and the obtained models for rat CPT I (*red*) and COT (*green*), showing the structural similarity between both threading-obtained models and the common template.

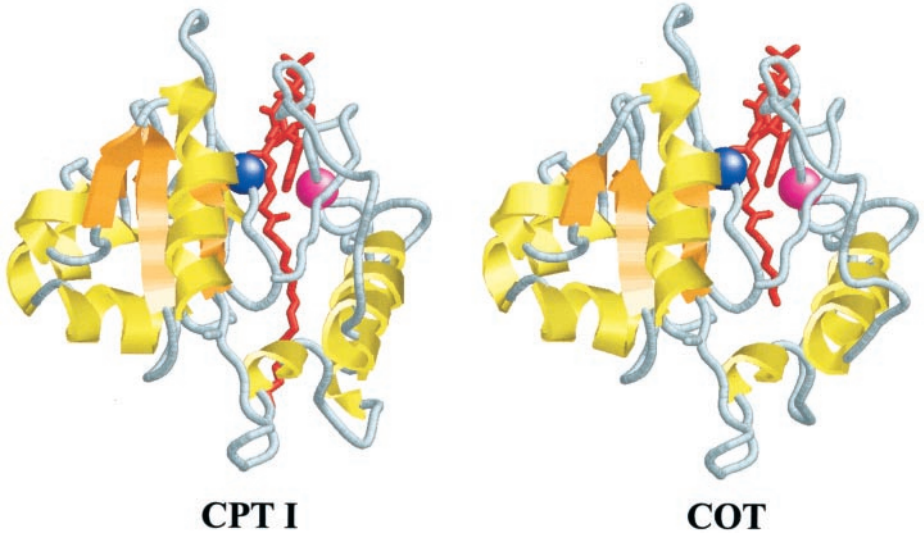

FIG. 3. **CPT I and COT structural models.** Shown is a *ribbon plot* representation of the proposed models for the catalytic surrounding regions of CPT I (*left*) and COT (*right*). β-Sheets are in *orange*, α-helices are in *yellow*. *Stick representations* of a molecule of palmitoyl-CoA (*left*) or octanoyl-CoA (*right*) are included, suggesting their putative locations at the active site. The positions of CPT I amino acids His^{473} (*blue*) and Ala^{381} (*magenta*) and their equivalent COT residues His^{327} (*blue*) and Ala^{238} (*magenta*) are also indicated as *colored spheres*.

Ala^{381} in CPT I or Ala^{238} in COT is conserved in all of the medium and long chain acyltransferases, being replaced by glycine in the short-chain actyltransferases (Fig. 4). The implicit importance of this position in the activity of the enzymes and their proximity to the active site led us to initiate a series of experiments to test this hypothesis. The loss of enzymatic activity of CPT I and COT mutants precisely in this position would support the structural model. It makes possible the assumption of the structural position of all of the amino acids of the central core of these proteins and future studies on the functionality of other residues as well as other enzymes belonging to this same family of proteins.

Generation of Mutations and Expression in S. cerevisiae—Plasmids carrying substitution mutations H473A and A381D in CPT I and H327A and A238D in COT were constructed as described under "Experimental Procedures." *S. cerevisiae* was chosen as an expression system because it does have neither endogenous CPT I nor COT activity. The pYES expression plasmid expressed CPT I and COT under the control of upstream activating and promoter sequences from *S. cerevisiae* and the *GAL1* gene for high level, tightly regulated transcription. Yeast transformants with the wild-type CPT I and COT genes and the mutants were grown in liquid medium described under "Experimental Procedures." CPT I and COT activity were absent in the control yeast strain transformed with the empty vector (data not shown).

Western blot analysis of wild-type CPT I and COT and the mutants using polyclonal antibodies directed against polypeptides from both proteins is shown in Fig. 5*B*. For the wild type and the two mutants, proteins of predicted sizes were synthesized with similar levels of expression.

Kinetics of Mutations on CPT I and COT Activities—Mutation H473A in CPT I, which was at the same homologous site as His^{327} in COT (12), completely abolished the enzyme activity (Fig. 5*A*). It was thus impossible to perform saturation kinetics and determine the K_m or the V_{max} values for carnitine or palmitoyl-CoA. Although Ala^{381} in CPT I is 92 amino acids away from the CPT I His^{473}, they are close in the structural model. The same happened in COT (Ala^{238} is 89 amino acids from His^{327}) but close in the model. So we mutated these alanines in both proteins and measured the catalytic activity. In case of an important decrease, the model would be supported.

The enzyme activity decreased by 86% in mutant CPT I A381D and by 80% in COT A238D (Fig. 5*A*). Both mutants showed normal saturation kinetics when the carnitine concentration was varied relative to a constant second substrate, either palmitoyl-CoA (in CPT I) or decanoyl-CoA (in COT), as did the wild-type CPT I and COT (Fig. 6). The K_m for palmitoyl-CoA as substrate increased from 4.9 to 33.3 μM in CPT I. An analogous change was seen for the K_m in COT (from 2 to 16.7 μM) (Table I). The K_m for carnitine changed less than for

```
                    *
CPT1_HUMAN  377 EARLAALTAGDRVPWARCRQ 396
CPT1_MOUSE  368 EAKLAALTAADRVPWAKCRQ 387
CPT1_RAT    377 EAKLAALTAADRVPWAKCRQ 396
CPTM_HUMAN  378 EEKLAALTAGGRVEWAQARQ 397
CPTM_RAT    378 EEKLAALTAGGRVEWAEARQ 397
CPT2_HUMAN  285 EFPLAYLTSENRDIWAELRQ 304
CPT2_MOUSE  285 EFPLAYLTSENRDVWAELRQ 304
CPT2_RAT    285 EFPVAYLTSENRDVWAELRQ 304
OCTC_HUMAN  234 GPGIAALTSEERTRWAKARE 253
OCTC_RAT    234 GPSIAALTSEERTRWAKARE 253
OCTC_BOVIN  234 GPGVAALTTEERTRWAKARE 253
CACP_HUMAN  245 KEPVGILTSNHRNSWAKAYN 264
CACP_MOUSE  246 KEPVGILTSNHRNTWAKAYN 265
CACP_COLLI  246 KEPVGILTTNHRNSWAKAYN 265
CLAT_HUMAN  347 LPPIGLLTSDGRSEWAEART 366
CLAT_MOUSE  239 LPPIGLLTSDGRSEWAKART 258
CLAT_RAT    238 LPPIGLLTSDGRSEWAKART 257
CLAT_PIG    239 LPPIGLLTSDGRSEWAEART 258
CLAT_DROME  306 PVPVGLLTAEPRSTWARDRE 325
```

FIG. 4. **A portion of the alignment of various carnitine/choline acyltransferases.** Amino acid sequence of representative members of the subfamilies carnitine palmitoyltransferase I from liver (*CPT1*) or muscle (*CPTM*), carnitine palmitoyltransferase II (*CPT2*), carnitine octanoyltransferase (*OCTC*), carnitine acetyltransferase (*CACP*), and choline acetyltransferase (*CLAT*) from several organisms (human, mouse, rat, bovine, pig, *Drosophila melanogaster* (*DROME*), and pigeon (*Columba livia*, *COLLI*)) were aligned using Clustal W (18). The selected region of the whole alignment contains a tree determinant position, indicated by an *asterisk*, between acetyltransferases (*CACP* and *CLAT*) and octanoyl and palmitoyltransferases (*OCTC* and *CPT1/M/2*), thus suggesting an active role for this position in the catalytic activity. Amino acid sequences are named and numbered according to the SWISS-PROT protein sequence data base (available on the World Wide Web at www.expasy.ch/sprot/). Residues are *colored* by conservation as in Fig. 1.

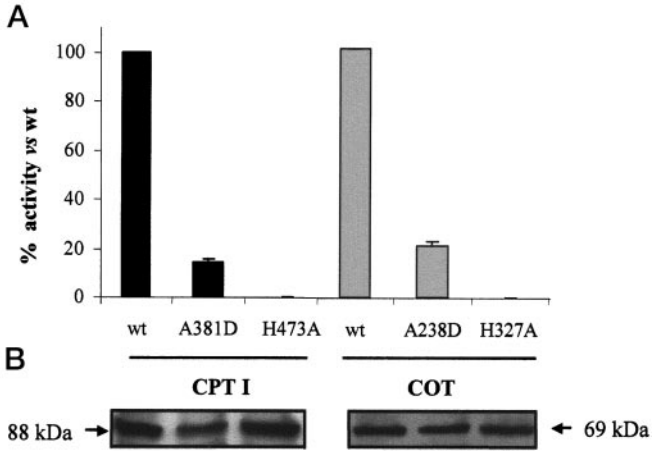

FIG. 5. *A*, relative activity of expressed wild-type and mutant CPT I and COT. Values (means ± S.D., $n = 3–5$) are taken from Table I. *B*, immunoblots showing expression of wild type and mutants of CPT I and COT. *S. cerevisiae* extracts (100 μg for CPT I and 10 μg for COT) were separated by SDS-PAGE and subjected to immunoblotting using specific antibodies. The *arrows* indicate the migration position and the molecular mass of rat liver CPT I and COT.

acyl-CoA. Mutant CPT I A381D had a K_m value of 93 μM (72% of the wild type), whereas mutant COT A238D had a K_m for carnitine of 146 μM, which was 85% of the wild-type (172 μM). The V_{max} changed slightly for both acyl-CoA and carnitine (Table I and Fig. 6). It is concluded that the mutation of alanine alters the K_m for fatty acyl-CoA (6.8–8.4-fold) more than V_{max} in the two enzymes.

Effect of Mutations on Malonyl-CoA Sensitivity—Substitution mutants CPT I A381D and COT A238D were measured for malonyl-CoA sensitivity, and the inhibition results were compared with those of wild-type (Fig. 7). Inhibition by malonyl-CoA in the range 1–200 μM was nearly identical in CPT I A381D and in the wild type. Analogous results were obtained with COT. Inhibition by malonyl-CoA in the range 1–200 μM was identical in mutant A238D and in control. These results

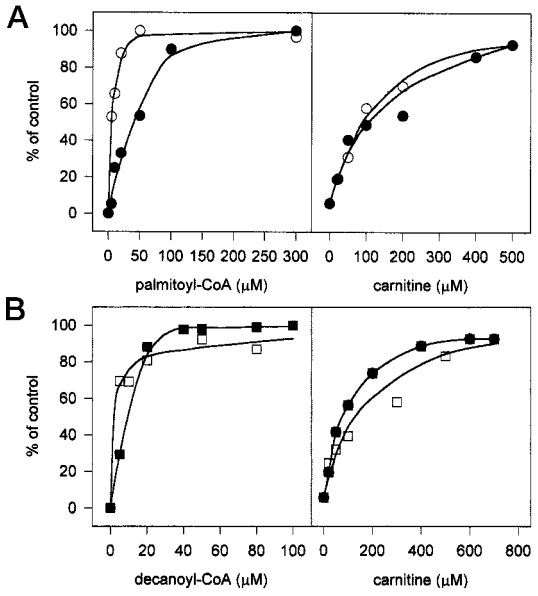

FIG. 6. *A*, kinetic analysis of the expressed wild-type CPT I and mutant A381D. Isolated mitochondria (10 μg of protein) from the yeast expressing the wild-type (○) and A381D mutant (●) were assayed for CPT activity in the presence of increasing concentrations of carnitine and palmitoyl-CoA. *B*, same as *A*, but for COT, wild type (□), and A238D mutant (■), using decanoyl-CoA as acyl-CoA substrate.

showed that although CPT I Ala^{381} and COT Ala^{238} are implicated in the catalytic activity, they do not participate in malonyl-CoA regulation.

Localization of Previous Described Mutations in the Structural Model—A positional study was performed with all the missense mutations in CPT I described so far included in the catalytic core studied (amino acids 368–567). The replacement of aspartic acid by glycine at position 454 produces human L-CPT I deficiency (42). This Asp^{454} together with Arg^{451} and Trp^{452}, which have been replaced by site-directed mutagenesis and produce an important loss of activity (13), are located in the model at the end of the cavity where the substrate palmitoyl-CoA is placed (Fig. 8). The artificial mutation W391A (13), which involves the loss of 51% of activity, is located within the channel of the substrate. The deletion mutant delR395 (43), producing hereditary L-CPT I deficiency, also located in the model, decreases the positive charge in the environment. The other two mutants reported by the same authors (P479L and L484P) lie in a domain, which is the opposite site in the channel to the CoA site of the substrate (facing toward the ω-methyl group of the acyl-CoA). Since mutant P479L decreases the sensitivity to malonyl-CoA, this domain may be the locus of inhibitor binding. The effect of mutant R388A (12) is not so evident in terms of alteration of the model. It is possible that the change of charge determines modifications of the tertiary structure of CPT I.

DISCUSSION

Despite efforts in biochemical characterization of carnitine palmitoyltransferases and their related enzymes, their mode of action is not completely understood, probably due to the lack of any structural characterization of the catalytic site. In the absence of an appropriate crystallized reference, some bioinformatics tools can be applied to obtain a structural model able to approximately address some important questions related to these proteins' activity.

The threading or "remote homology design" is a three-dimensional structure prediction technique useful when there is not enough sequence similarity of the input sequence and a known three-dimensional structure and, therefore, the "homology

TABLE I

Carnitine acyltransferase activity and kinetic parameters in yeast strains expressing wild-type and mutant CPT I and COT

Extracts from yeast expressing wild type and histidine and alanine substitution mutations of CPT and COT were assayed for activity and kinetics as described under "Experimental Procedures." The acyl-CoA substrate was palmitoyl-CoA for CPT I and decanoyl-CoA for COT. The results are the means ± S.D. of at least three independent experiments with different preparations. WT, wild type; ND, not determined.

Strain	Activity	Acyl-CoA		Carnitine	
		K_m	V_{max}	K_m	V_{max}
	nmol/min·mg				
CPTI (WT)	17.7 ± 0.9	4.9 ± 0.3	6.3 ± 0.4	127.4 ± 4	6.6 ± 0.8
CPTI H473A	ND	ND	ND	ND	ND
CPTI A381D	2.5 ± 0.3	33 ± 8	5.9 ± 0.2	93 ± 5	2.9 ± 0.4
COT (WT)	226 ± 9	2.0 ± 0.2	67 ± 4	172 ± 46	205 ± 24
COT H327A	ND	ND	ND	ND	ND
COT A238D	47 ± 5	16.7 ± 0.7	100 ± 12	146 ± 10	124 ± 10

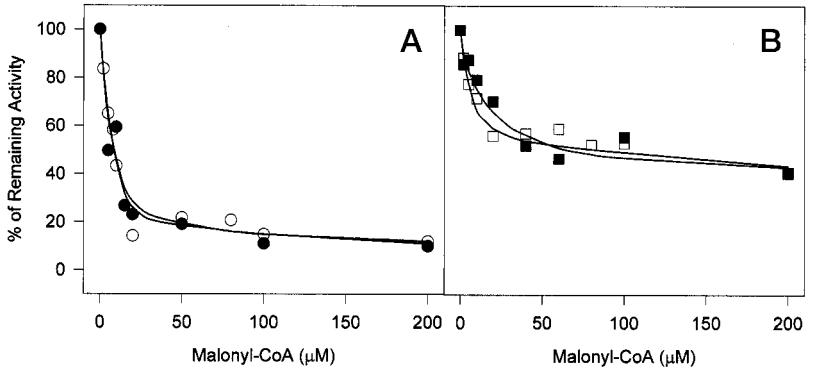

FIG. 7. **Effect of malonyl-CoA on the activity of wild type and mutants of CPT I and COT.** The mean data from three to four curves obtained from separate yeast expressions are shown. *A*, 10 μg of mitochondria from *S. cerevisiae* expressing CPT I wild-type (○) and A381D mutant (●) were assayed for CPT activity in the presence of increasing concentrations of malonyl-CoA (1–200 μM). *B*, 2 μg of *S. cerevisiae* extracts expressing COT wild-type (□) and A238D mutant (■) were assayed for COT activity in the presence of increasing concentrations of malonyl-CoA (1–200 μM).

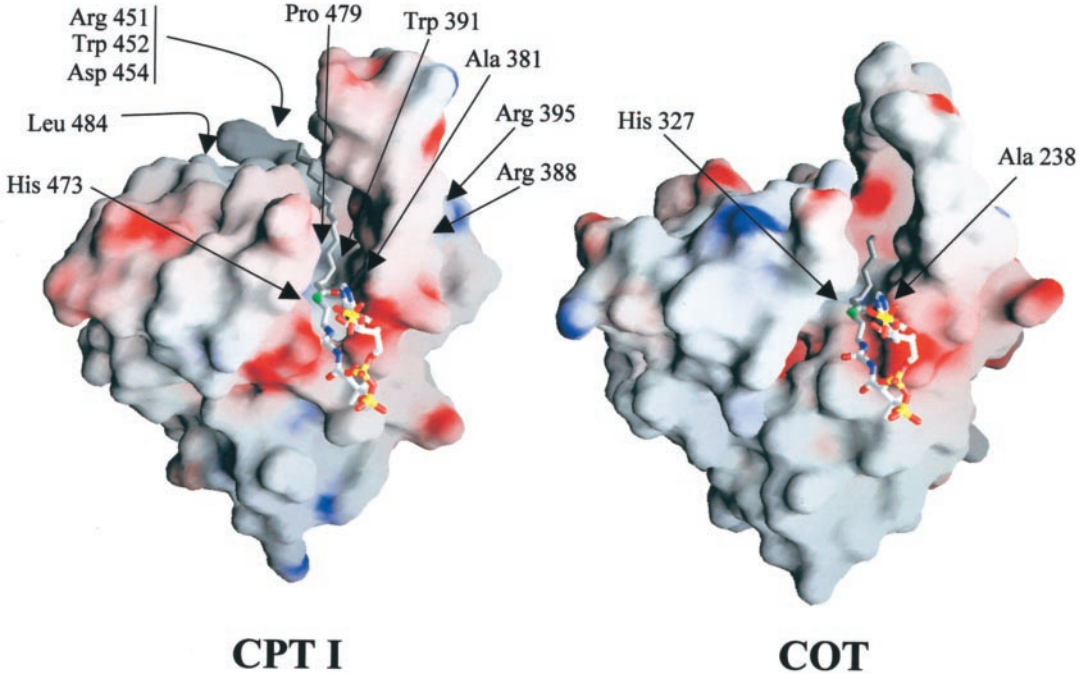

FIG. 8. **Solvent-accessible surface representation of the proposed models for CPT I (*left*) and COT (*right*).** The surface of both models is colored as in Fig. 1. Schematic structure of the proposed substrate positions is represented. The approximate locations of some amino acid residues whose mutation decreases enzyme activity, are also indicated by *arrows*. Note the proximity of His^{473} and Ala^{381} (CPT I, *left*) or His^{327} and Ala^{238} (COT, *right*) to the sulfur atom (*green stick*) of the respective acyl-CoA substrate.

modeling" is not applicable. The process adapts the sequence to different known foldings and evaluates the fitting. The meaning of "fitting" varies from one threading program to others: secondary structure coincidence, similar accessibility, or solvatation energy, etc. Methods of protein fold recognition attempt to detect similarities between protein three-dimensional structure that are not accompanied by any significant sequence similarity. There are many approaches, but the unifying theme

is to try and find folds that are comparable with a particular sequence. Unlike sequence-only comparison, these methods take advantage of the extra information made available by three-dimensional structural data.

To detect structural homologies between CPT I and COT and any other three-dimensional representation, we used an integrative approach of two programs, THREADER2 (22) and FUGUE threading server (23). Whereas the first one uses solvatation potentials and predicted contacts, the latter performs a fold recognition analysis using structural environment-specific substitution tables and structure-dependent gap penalties. The integration of both methodologies revealed that the three-dimensional fold of the central site of all acyl-CoA transferases can be structured in the same way as the enoyl-CoA hydratase monomer (Protein Data Bank entry 2dub, chain E). What was more important was to observe that CPT I and COT had nearly identical structural models for the central region, which putatively contains the catalytic site (amino acids 368–567 of CPT I and amino acids 226–417 of COT). The predicted secondary structure for the 200 amino acids that putatively contains the palmitoyl-CoA or decanoyl-CoA binding region consists of 6 α-helices and 4 β-sheets.

Additional support of this fold as template is based on the fact that these proteins bind very similar ligands, all of them acyl-CoA derivatives; the crystal structure of the enoyl-CoA hydratase monomer includes precisely a molecule of octanoyl-CoA, used as inhibitor in this case, the natural substrate of COT. Enoyl-CoA hydratase (Protein Data Bank code 2dub), also known as crotonase, belongs to the enoyl-CoA hydratase/isomerase family. It is a homohexameric enzyme, located at the mitochondrial matrix. It catalyzes the second step in the mitochondrial fatty acid β-oxidation pathway, transforming the 3-hydroxyacyl-CoA into *trans*-2(or 3)-enoyl-CoA plus H_2O.

The model predicts that although CPT I Ala^{381} (Ala^{238} in COT) is 92 amino acids away from the CPT I His^{473} (His^{327} in COT) it is very close to the catalytic histidines. The important decrease in activity (14–20% of residual activity with respect to the wild type) after mutation CPT I A381D or COT A238D confirms the function of these alanines and supports the three-dimensional model. The marked modification of K_m for acyl-CoA of the mutants supports the role of these alanines in locating the substrates to the catalytic site.

In addition, these alanine residues had been implicated in CPT and COT activity by a tree determinant study of the complete alignment of the carnitine-choline acyltransferase family of proteins. In a protein family alignment, the positions considered as tree determinants, or subfamily conserved residues, are usually accepted to be implicated in key catalytic activities, being responsible for the different substrate specificities or enzymatic activities of the different subfamilies of the alignment (37, 38). A clear example of this type of analysis was made previously in this same family of proteins related to the carnitine *versus* choline affinity (44). The structure-based alignment of the template sequence with all the other transferases sequences used in the extensive threading procedure can also be used to build three-dimensional models of all the other members of the family in the future.

The group of Woldegiorgis (13) suggested that the region comprised between 381–481 could be the putative palmitoyl-CoA binding site. Moreover, the abolition of activity after mutation of H473A strongly suggests that this His^{473} is the catalytic site. McGarry and co-workers (11), after mutagenesis of homologous histidine in CPT II, proposed that this was the catalytic site. This was confirmed in a previous study in COT, in which mutant H327A abolished the catalytic activity (45). Dai *et al.* (13) questioned whether these histidines were the catalytic sites after the observation that chemical modification of mitochondria from yeast strains expressing L-CPT I and M-CPT I by diethylpyrocarbonate had no effect on catalytic activity. It is possible that expressed CPT I in yeast mitochondria makes this histidine inaccessible for diethylpyrocarbonate modification. Brown *et al.* (11) suggested that a charge-relay system involving this His coupled with an Asp extracts a proton from the C-3 hydroxyl group of carnitine, allowing for nucleophilic attack of the resulting oxyanion of the carbonyl group of the acyl-CoA thioester. Site-directed mutagenesis experiments in carnitine acetyltransferase supports this model, which tends to exclude a modified enzyme intermediate from the reaction pathway (46).

The question of whether the substrates of carnitine acyltransferases bind to the same locus as malonyl-CoA has been subject of much discussion. Under this view, malonyl-CoA could be a competitive inhibitor of palmitoyl-CoA as substrate in CPT I. Whereas mutation of A381D (in the middle of the catalytic channel) strongly decreases catalytic activity, it does not modify the inhibition to malonyl-CoA in the range 1–200 μM in CPT I and in COT. These specific mutants behave similarly to the mutants reported in Ref. 13, since in most of them the capacity of malonyl-CoA to inhibit the mutated enzymes is maintained. On the contrary, natural mutant P479L (43), located in a domain that is facing toward the middle of the substrate-binding channel, has decreased sensitivity to malonyl-CoA, whereas the CPT I activity is not severely decreased (21.6% residual activity). Therefore, Ala^{381}, although located in the model near Pro^{479}, appears not to mediate the malonyl-CoA inhibitory effect, suggesting fine interactions in the amino acids involved in the binding of malonyl-CoA.

Mutation of residues described previously also supports the model: amino acids Trp^{391}, Arg^{451}, Trp^{452} (13), and Asp^{454} (42), because they are in the channel in which substrates are fitted in the catalytic event, and the amino acids Arg^{388} and Arg^{395} (13), located in the neighborhood of the catalytic channel, because the change in charge probably disrupts the delicate charge environment. Mutant L484P (43) is also present at the end of the catalytic channel, which confirms the absence of activity. The similar trace of the amino acid backbone of enoyl-CoA hydratase (determined by x-ray), the location in the model of amino acids previously shown as important in the catalytic event and the functional location of alanines, predicted to be placed at least 4 Å from the catalytic histidine in CPT I and COT confirm the model. This model will facilitate in the future the studies of interaction of the substrates (palmitoyl-CoA or octanoyl-CoA) or the physiological inhibitor, malonyl-CoA, with CPT I and COT and their role in the physiological regulation of fatty acid β oxidation.

Acknowledgments—We are grateful to Dr. V. Zammit, who kindly provided the CPT I antibodies. We are also grateful to Robin Rycroft of the Language Service for valuable assistance in the preparation of the English manuscript.

REFERENCES

1. Esser, V., Britton, C. H., Weis, B. C., Foster, D. W., and Mc Garry, J. D. (1993) *J. Biol. Chem.* **268,** 5817–5822
2. Britton, C. H., Schultz, R. A., Zhang, B., Esser, V., Foster, D. W., and McGarry, J. D. (1995) *Proc. Natl. Acad. Sci. U. S. A.* **92,** 1984–1988
3. Yamazaki, N., Shinohara, Y., Shima, A., Yamanaka, Y., and Terada, H. (1996) *Biochim. Biophys. Acta* **1307,** 157–161
4. Yamazaki, N., Shinohara, Y., Shima, A., and Terada, H. (1995) *FEBS Lett.* **363,** 41–45
5. McGarry, J. D., and Brown, N. F. (1997) *Eur. J. Biochem.* **244,** 1–14
6. A'Bhaird, N. N., and Ramsay, R. R. (1992) *Biochem. J.* **286,** 637–640
7. Fraser, F., Corstorphine, C. G., and Zammit, V. A. (1997) *Biochem. J.* **323,** 711–718
8. Jackson, V. N., Cameron, J. M., Fraser, F., Zammit, V. A., and Price, N. T. (2000) *J. Biol. Chem.* **275,** 19560–19566
9. van der Leij, F. R., Huijkman, N. C., Boomsma, C., Kuipers, J. R., and Bartelds, B. (2000) *Mol. Genet. Metab.* **71,** 139–153
10. Schmalix, W., and Bandlow, W. (1993) *J. Biol. Chem.* **268,** 27428–27439

11. Brown, N. F., Anderson, R. C., Caplan, S. L., Foster, D. W., and McGarry, J. D. (1994) *J. Biol. Chem.* **269,** 19157–19162
12. Morillas, M., Clotet, J., Rubí, B., Serra, D., Asins, G., Ariño, J., and Hegardt F. G. (2000) *FEBS Lett.* **466,** 183–186
13. Dai, J. Zhu, H., Shi, J., and Woldegiorgis, G. (2000) *J. Biol. Chem.* **275,** 22020–22024
14. Nic a'Bhaird, N., Yankovskaya, V., and Ramsay, R. R. (1998) *Biochem. J.* **330,** 1029–1036
15. Cronin, C. N. (1997) *Eur. J. Biochem.* **247,** 1029–1037
16. Engel, C. K., Kiema, T. R., Hiltunen, J. K., and Wierenga, R. K. (1998) *J. Mol. Biol.* **275,** 847–859
17. Altschul, S. F., Gish, W., Miller, W., Myers, E. W., and Lipman, D. J. (1990) *J. Mol. Biol.* **215,** 403–410
18. Thompson, J. D., Higgins, D. G., and Gibson, T. J. (1994) *Nucleic Acids Res.* **22,** 4673–4680
19. Rost, B. (1996) *Methods Enzymol.* **266,** 525–539
20. Cuff, J. A., Clamp, M. E., Siddiqui, A. S., Finlay, M., and Barton, G. J. (1998) *Bioinformatics* **14,** 892–893
21. Jones, D. T., Tress, M., Bryson, K., and Hadley, C. (1999) *Proteins* **37,** 104–111
22. Jones, D. T., Miller, R. T., and Thornton, J. M. (1995) *Proteins* **23,** 387–397
23. Shi, J., Blundell, T. L., and Mizuguchi, K. (2001) *J. Mol. Biol.* **310,** 243–257
24. Orengo, C. A., Michie, A. D., Jones, S., Jones, D. T., Swindells, M. B., and Thornton, J. M. (1997) *Structure* **5,** 1093–1108
25. Holm, L., and Sander, C. (1996) *Nucleic Acids Res.* **24,** 206–210
26. Murzin, A., Brenner, S. E., Hubbard, T., and Chothia, C. (1995) *J. Mol. Biol.* **247,** 536–540
27. Guex, N., Peitsch, M. C. (1997) *Electrophoresis* **18,** 2714–2723
28. Guex, N., Diemand, A., and Peitsch, M. C. (1999) *Trends Biochem. Sci.* **24,** 364–367
29. Peitsch, M. C. (1995) *Bio/Technology* **13,** 658–660
30. Peitsch, M. C. (1996) *Biochem. Soc. Trans.* **24,** 274–279
31. Sippl, M. J. (1993) *Proteins* **17,** 355–362
32. Hooft, R. W., Vriend, G., Sander, C., and Abola, E. E. (1996) *Nature* **381,** 272
33. Vriend, G. (1990) *J. Mol. Graph.* **8,** 52–56
34. Laskowski, R. A., MacArthur, M. W., Moss, D. S., and Thornton, J. M. (1993) *J. Appl. Crystallogr.* **26,** 283–291
35. Nicholls, A., Bharadwaj, R., and Honig, B. (1993) *Biophys. J.* **64,** 166 (abstr.)
36. Sayle, R. A, and Milner-White, E. J. (1995) *Trends Biochem. Sci.* **20,** 374
37. Casari, G., Sander, C., and Valencia, A. (1995) *Nat. Struct. Biol.* **2,** 171–178
38. Pazos, F., Sanchez-Pulido, L., García-Ranea, J. A., Andrade, M. A., Atrian, S., and Valencia A. (1997) in *Biocomputing and Emergent Computation* (Lundh, D., Olsson, B., and Narayanan, A., eds) pp. 132–145, World Scientific, Singapore
39. Datta, A. K. (1995) *Nucleic Acids Res.* **23,** 4530–4531
40. Schiestl, R. H., and Gietz, R. D. (1989) *Curr. Genet.* **16,** 339–346
41. Sherman, F., Fink, G. R., and Hicks, J. B. (1986) *Laboratory Course Manual for Methods in Yeast Genetics*, Cold Spring Harbor Laboratory, Cold Spring Harbor, NY
42. Ijist, L., Mandel, H., Oostheim, W., Ruiter, J. P., Gutman, A., and Wanders, R. J. (1998) *J. Clin. Invest.* **102,** 527–531
43. Brown, N. F., Mullur, R. S., Subramanian, I., Esser, V., Bennett, M. J., Saudubray, J. M., Feigenbaum, A. S., Kobari, J. A., Macleod, P. M., McGarry, J. D., and Cohen, J. C. (2001) *J. Lipid Res.* **42,** 1134–1142
44. Cronin, C. N. (1998) *J. Biol. Chem.* **273,** 24465–24469
45. Morillas, M., Clotet, J., Rubí, B., Serra, D., Ariño, J., Hegardt, F. G., and Asins, G. (2000) *Biochem. J.* **351,** 495–502
46. Cronin, C. N. (1997) *Biochem. Biophys. Res. Commun.* **238,** 784–789; Correction (1997) *Biochem. Biophys. Res. Commun.* **247,** 803–804
47. Sander, C., and Schneider, R. (1991) *Proteins* **9,** 56–68